Received: 23 April 2020 | Revised: 24 August 2020 | Accepted: 25 August 2020

DOI: 10.1111/mpp.12996

ORIGINAL ARTICLE

Molecular Plant Pathology | WILEY

At the scene of the crime: New insights into the role of weakly pathogenic members of the fusarium head blight disease complex

Jiang Tan[1] | Maarten Ameye[1] | Sofie Landschoot[1] | Noémie De Zutter[1] | Sarah De Saeger[2] | Marthe De Boevre[2] | Mohamed F. Abdallah[1,2] | Theo Van der Lee[3] | Cees Waalwijk[3] | Kris Audenaert[1]

[1]Laboratory of Applied Mycology and Phenomics, Department of Plants and Crops, Faculty of Bioscience Engineering, Ghent University, Ghent, Belgium

[2]Centre of Excellence in Mycotoxicology and Public Health, Department of Bioanalysis, Faculty of Pharmaceutical Sciences, Ghent University, Ghent, Belgium

[3]Wageningen University and Research Centre, Wageningen, Netherlands

Correspondence
Maarten Ameye, Laboratory of Applied Mycology and Phenomics, Department of Plants and Crops, Faculty of Bioscience Engineering, Valentin Vaerwyckweg 1, B-9000, Ghent University, Ghent, Belgium.
Email: maarten.ameye@ugent.be

Funding information
Bijzonder Onderzoeksfonds

Abstract

Plant diseases are often caused by a consortium of pathogens competing with one another to gain a foothold in the infection niche. Nevertheless, studies are often limited to a single pathogen on its host. In Europe, fusarium head blight (FHB) of wheat is caused by multiple *Fusarium* species, including *Fusarium graminearum* and *F. poae*. Here, we combined a time series of (co)inoculations, monitored by multispectral imaging, transcriptional, and mycotoxin analyses, to study the temporal interaction between both species and wheat. Our results showed coinoculation of *F. graminearum* and *F. poae* inhibited symptom development but did not alter mycotoxin accumulation compared to a single inoculation with *F. graminearum*. In contrast, preinoculation of *F. poae* reduced both FHB symptoms and mycotoxin levels compared to a single *F. graminearum* infection. Interestingly, *F. poae* exhibited increased growth in dual infections, demonstrating that this weak pathogen takes advantage of its co-occurrence with *F. graminearum*. Quantitative reverse transcription PCR revealed that *F. poae* induces *LOX* and *ICS* gene expression in wheat. We hypothesize that the early induction of salicylic and jasmonic acid-related defences by *F. poae* hampers a subsequent *F. graminearum* infection. This study is the first to report on the defence mechanisms of the plant involved in a tripartite interaction between two species of a disease complex and their host.

KEYWORDS

disease complex, *Fusarium*, multispectral imaging, plant–pathogen interaction, wheat

1 | INTRODUCTION

Plant diseases have been studied for decades as the interaction of a single pathogen with its host. However, it is now being recognized that plant diseases are often the result of multispecies interactions, including two or more pathogens from the same or even different kingdoms (Lamichhane and Venturi, 2015). Fusarium head blight (FHB) is one of the most important fungal diseases on wheat, causing

Jiang Tan and Maarten Ameye contributed equally to this work.

yield losses of up to 40% (Parry *et al*., 1995). Although the hemibiotrophic fungus *Fusarium graminearum* sensu stricto (O'Donnell *et al*., 2004) is considered to be the primary causal agent of the disease in central Europe, North America, and Asia (Leplat *et al*., 2013; Backhouse, 2014), several species involved in FHB are frequently reported. In Europe, besides *F. graminearum*, *F. culmorum*, *F. poae*, *F. avenaceum*, *Microdochium nivale*, and *M. majus* are the predominant species (Ioos *et al*., 2005; Xu *et al*., 2005). Despite their presence in association with diseased kernels, only *F. graminearum* and *F. culmorum* are considered highly pathogenic. The other species are less aggressive on wheat in that they may infect but do not proliferate, grow superficially, or only thrive at the sites of inoculation (Stack and McMullen, 1985; Brennan *et al*., 2003).

In the interaction with wheat, *F. graminearum* first grows on the exterior parts of florets and glumes or between the cuticule and the epidermal cell wall (Bushnell *et al*., 2003). Finally, plant tissues are penetrated and the fungus spreads throughout the ear via the vascular system in the rachilla and rachis (Brown *et al*., 2010). This spread is facilitated via the production of the mycotoxin deoxynivalenol (DON) and its acetylated derivatives 3-acetyl DON and 15-acetyl DON, an important virulence factor causing necrosis of the ear tissue (Audenaert *et al*., 2014). During infection, *F. graminearum* corrupts the plant's defence system by reducing the expression of defence genes and boosts its DON production in response to the plant's oxidative burst, which is a typical hallmark of first-line plant defence (Desmond *et al*., 2008; Audenaert *et al*., 2014). A successful plant defence against *F. graminearum* is meticulously regulated by a sequential defence signalling comprising salicylic acid (SA) and jasmonic acid (JA) during the early and later stages of infection, respectively (Ameye *et al*., 2015).

An important but more enigmatic member of the FHB complex is *F. poae*. Compared to other *Fusarium* members of the FHB disease complex, *F. poae* causes the least reduction of seed germination, hence *F. poae* can be considered a weak pathogen compared to other *Fusarium* species (Browne and Cooke, 2005). Despite its low virulence, *F. poae* is omnipresent in Europe (Xu *et al*., 2005; Audenaert *et al*., 2009; Vogelgsang *et al*., 2019), which is partially attributed to its higher resistance to fungicides compared to other *Fusarium* species. Treating wheat fields with azole fungicides causes the *Fusarium* population to shift from a population dominated by *F. culmorum* and *F. graminearum* to a *F. poae*-dominated population (Audenaert *et al*., 2011). *F. poae* produces a complex blend of both type A (diacetoxyscirpenol [DAS] and neosolaniol [NEO]) and type B (nivalenol [NIV] and fusarenon-x [FUS-X]) trichothecenes whose function remains enigmatic (Sugiura *et al*., 1993; Thrane *et al*., 2004; Vogelgsang *et al*., 2008; Vanheule *et al*., 2017). However, no *F. poae* isolate has been identified that produces the virulence factor DON or its acetylated derivatives 3-acetyl DON and 15-acetyl DON, which are produced by the more aggressive pathogens in the FHB complex such as *F. graminearum*, *F. culmorum*, or *F. asiaticum*.

In this study, we hypothesized that *F. poae* depends on the presence of *F. graminearum* to infect wheat and that the presence of *F. poae* influences the disease symptom development of *F. graminearum* in a time-dependent manner. However, using an approach of time series coinoculations combined with phenomics and transcript analyses, we could demonstrate that the interaction between both species of the FHB disease complex is far more complex, with highly divergent symptoms depending on the timing of inoculation. Our results show that *F. poae* primes plant defence, which hampers subsequent infection by *F. graminearum*. Moreover, *F. poae* takes advantage of its co-occurrence with the highly virulent *F. graminearum*. Our study demonstrates that *F. poae* is a freerider rather than an innocent bystander at the FHB infection site.

2 | RESULTS

2.1 | In the field, *F. poae* and *F. graminearum* co-occur in the same spikelets

By analysing the data of a 17-year survey in seven locations scattered throughout Flanders, Belgium, we assessed the co-occurrence of *F. poae* and *F. graminearum*. In total, more than 7,000 wheat ears and more than 40 cultivars were assessed for the presence of FHB members. This analysis showed that in the ears with symptoms *F. poae* occurred in 30.0% of the cases alone, in 31.2% *F. poae* co-occurred with *F. graminearum*, and in 15.4% *F. poae* co-occurred with *F. graminearum* and *F. culmorum* (Figure 1a,b). This multiyear, multilocation analysis showed a significant co-occurrence of *F. poae* with *F. graminearum* and *F. avenaceum* under field conditions (Figure 1c). Because of the low incidence of *F. avenaceum*, we did not further focus on the interaction with this species.

2.2 | Impact of *F. poae* on *F. graminearum* disease progression on detached wheat leaves

To investigate the co-occurrence of *F. poae* and *F. graminearum* in the field, we used a previously established model system of detached wheat leaves (Ameye *et al*., 2015) to assess symptom development of green fluorescent protein (GFP)-tagged *F. graminearum* PH-1 and wild-type *F. poae* 2516. To assess whether preinoculation of *F. poae* affected the outcome of the *F. graminearum* infection, we inoculated a *F. poae* conidial suspension one day before the *F. graminearum* inoculation. Remarkably, the preinoculation with *F. poae* resulted in complete abolition of *F. graminearum* disease symptom development and the phenotype of no necrotic lesions on the leaf resembled that of a singular *F. poae* infection. This phenotype of no necrotic lesions was confirmed by the efficiency of photosystem II F_V/F_M values that reflect the healthy condition of leaf. The F_V/F_M values of preinoculation with *F. poae* were significantly higher than in the single *F. graminearum* inoculation (Figures 2a,b and S1). In addition, the lack of symptoms coincided with a decreased corrected (c)GFP signal, reflecting reduced presence of *F. graminearum* (Figure 2a,c) and a significant decrease in *F. graminearum* biomass (Figures 2d, S1, and S2). Finally, the typical reddish colour attributed to the presence

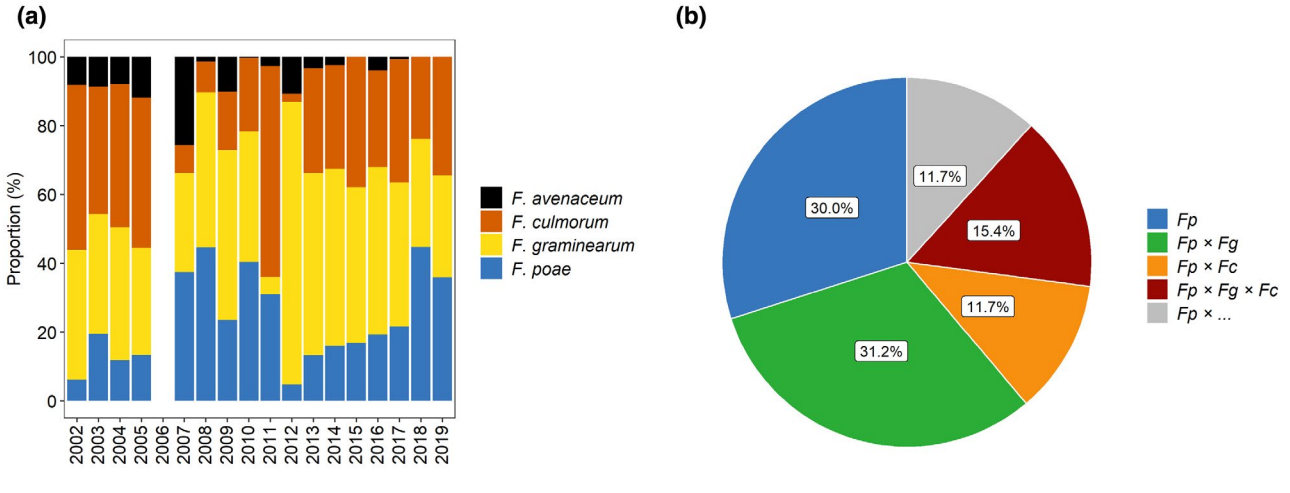

(c)

F. poae +	Species co-occurence	Number of observations	Number of co-occurences with *F. poae*	P (lower frequency)	P (higher frequency)
F. avenaceum	Positive	213	111	1.00	0.00
F. culmorum	Random	805	217	0.64	0.39
F. graminearum	Positive	1220	373	1.00	0.00

FIGURE 1 Presence of *Fusarium poae* alone or in combination with other *Fusarium* species on the same spikelets in field samples. (a) Prevalence of different *Fusarium* species in a large-scale investigation from 2002 until 2019. For 2006, no ears with symptoms were found during the period of sampling, hence no data are present. (b) Species association with *F. poae*. Fp, percentage of samples only containing *F. poae* and no other *Fusarium* species; Fp × Fg, percentage of samples containing both *F. poae* and *Fusarium graminearum* (and possibly also *Fusarium avenaceum* and/or *Microdochium nivale*); Fp × Fc, percentage of samples containing both *F. poae* and *Fusarium culmorum* (and possibly also *F. avenaceum* and/or *M. nivale*), Fp × Fg ×Fc, percentage of samples containing *F. poae*, *F. culmorum*, and *F. graminearum* (and possibly also *F. avenaceum* and/or *M. nivale*); Fp × ..., percentage of samples containing *F. poae*, *F. avenaceum*, and/or *M. nivale* (but no *F. graminearum* or *F. culmorum*). (c) Pairwise species co-occurrence patterns between *F. poae* and *F. avenaceum*, and *F. culmorum* and *F. graminearum*. exp_cooccur, expected number of sites having both species; P (lower frequency), probability that the two species would co-occur at a frequency less than the observed number of co-occurrence sites if the two species were distributed randomly (independently) of one another; P (higher frequency), probability of co-occurrence at a frequency greater than the observed frequency (Griffith *et al*., 2016)

of rubrofusarin, which is produced during an infection by *F. graminearum*, also disappeared when detached leaves were preinoculated with *F. poae* (Figure S3).

In the singular *F. graminearum* (w + g) inoculation, water-soaked lesions developed and extended from day 2 onwards, which resulted in a decrease of the maximum F_V/F_M compared to the mock-inoculated control leaves (Figures 2a,b and S4). In the singular *F. poae* (w + p) infection, no symptoms developed and F_V/F_M values of the detached leaves inoculated with *F. poae* were not significantly different from the mock-inoculated with water leaves (Figure S4), which demonstrates that *F. poae* cannot cause symptoms on its own (Figure 2a,b). In the dual inoculations in which *F. poae* and *F. graminearum* were inoculated at the same time, symptoms were significantly less severe compared to the single *F. graminearum* infection. These results were confirmed by assessing the presence and activity of *F. graminearum* visualized by the cGFP signal and its biomass assessed by quantitative reverse transcription PCR (RT-qPCR). Both parameters showed significant and a slight reduction respectively at day 3 compared to a singular infection with *F. graminearum* (Figure 2c,d). To assess whether there is direct antagonism between *F. poae* and *F. graminearum* in vitro, we coinoculated both species on potato dextrose agar (PDA) plates and no obvious mutual antagonism was observed (Figure S5).

To understand the impact of *F. graminearum* PH-1 on the presence of *F. poae* 2,516 we used a GFP-tagged *F. poae* 2,516 isolate in combination with a wild-type *F. graminearum* PH-1 and assessed the impact of the latter on *F. poae* presence. These experiments showed that a singular *F. poae* infection resulted in less *F. poae* biomass at day 3 (Figure 3a–c) and a reduced cGFP signal at day 4 compared to the leaves in which *F. poae* was inoculated with *F. graminearum* at same time (Figure S6). We inoculated the GFP-tagged *F. poae* on leaves which were mechanically wounded by scratching the epidermal layer over a length of 0.1, 1 and 2 cm with a sterile scalpel to check whether *F. poae* benefits from the leaf damage induced by *F. graminearum* infection. *F. poae* showed a significantly larger growth in larger wounds (Figure S7).

Finally, we monitored disease progress of *F. graminearum* by inoculating *F. poae* 1 or 2 days after *F. graminearum*. The *F. poae* inoculation did not influence the symptom development of *F. graminearum* in this experiment (Figure S8).

To verify our observations in wheat ears, the main niche of FHB pathogens, we assessed whether preinoculation of *F. poae* also reduced the infection of *F. graminearum* on ears. We therefore inoculated a *F. poae* conidial suspension 1 or 2 days before inoculating the same spikelets with *F. graminearum*. After 7 days of infection,

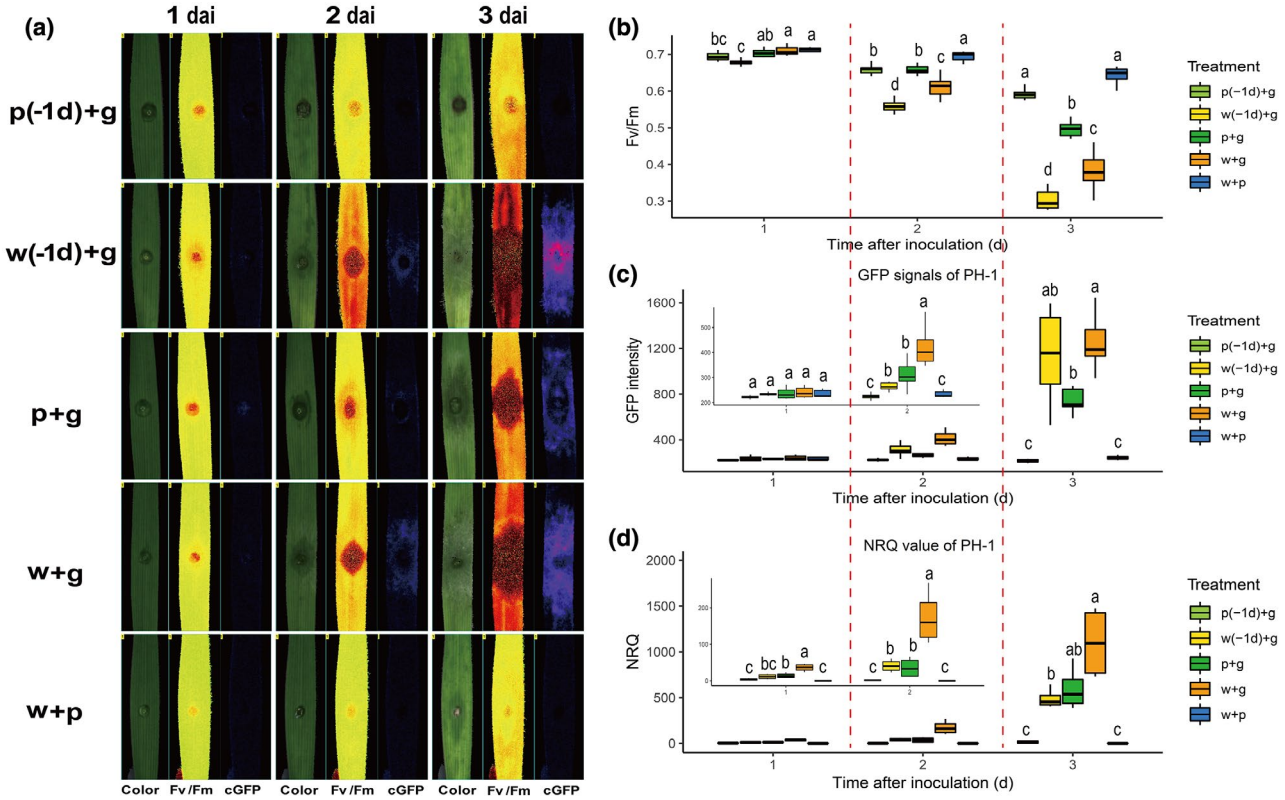

FIGURE 2 Impact of *Fusarium poae* 2,516 inoculation on *Fusarium graminearum* PH-1 infection in a detached leaf assay. (a) Pictures taken at three time points after infection (1, 2, and 3 days after inoculation [dai]). p(−2d) + g, preinoculation with *F. poae* 2,516 2 days before *F. graminearum* PH-1 inoculation; w(−2d) + g, preinoculation with water 2 days before *F. graminearum* PH-1 inoculation; p(−1d) + g, preinoculation with *F. poae* 2,516 1 day before *F. graminearum* PH-1 inoculation; w(−1d) + g, preinoculation with water 1 day before *F. graminearum* PH-1 inoculation; p + g, inoculation with *F. poae* 2,516 and *F. graminearum* PH-1 at the same time; w + g, inoculation with water and *F. graminearum* PH-1 at the same time; w + p, inoculation with water and *F. poae* 2,516 at the same time. (b) F_V/F_M (efficiency of photosystem II) values from 1 to 3 dai, $n = 8$. (c) Corrected green fluorescent protein (GFP) value from the GFP expressing PH-1 strain signal from 1 to 3 dai, $n = 8$. (d) Normalized quantitative relative values (NRQ) of *F. graminearum* PH-1 biomass, $n = 4$. Boxplots indicate the median (horizontal lines), 25th and 75th percentile range (boxes), and up to 1.5× interquartile range (whiskers). Different letters indicate significant differences between treatments ($p < .05$) for each time point

preinoculation of spikelets with *F. poae* 1 or 2 days before *F. graminearum* resulted in a not statistically significant trend of a decrease of FHB symptoms in ears, as measured by red-green-blue (RGB) images, higher F_V/F_M values (Figures 4a,b and S9), the percentage of low scored symptom ears (Figure 4d), a reduced cGFP signal of *F. graminearum* (Figures 4a,c and S9), and a reduction in *F. graminearum* biomass by RT-qPCR (Figures 4e and S9) compared to singular inoculation of *F. graminearum* or coinoculation of *F. graminearum* and *F. poae*, confirming our findings from the detached leaf assays.

2.3 | Gene expression analysis of trichothecene production

We analysed transcripts of the *TRI5* gene in *F. graminearum*, a key gene in DON biosynthesis. Both in the wheat leaf assay and in wheat ear assay, preinoculation with *F. poae* 1 or 2 days before inoculation with *F. graminearum* resulted in a significantly lower level of *TRI5* gene expression compared to a singular *F. graminearum* inoculation at early infection time points (days 1 and 2; Figures 5a,c and S10). At later time points (day 3 for leaves assay, days 4 and 7 for ears assay), the differences of *TRI5* gene relative expression between treatments was less pronounced except for the interaction in which *F. poae* was inoculated 2 days before an inoculation with *F. graminearum* and the interaction in which both of the species were inoculated at the same time in the leaf assay. For the *TRI5* gene expression in *F. poae*, the biomass of *F. poae* is very low and the expression of *TRI5* was below the detection level.

2.4 | Effect of *F. poae* on the production of type B trichothecenes during *F. graminearum* infection in detached leaves and ears

To assess the impact of *F. poae* on the presence of the type B trichothecenes produced by *F. graminearum* (DON, 15-ADON, and 3-ADON), these mycotoxins were quantitatively determined in leaves and ears at the end of the experiment at 4 and 7 days, respectively,

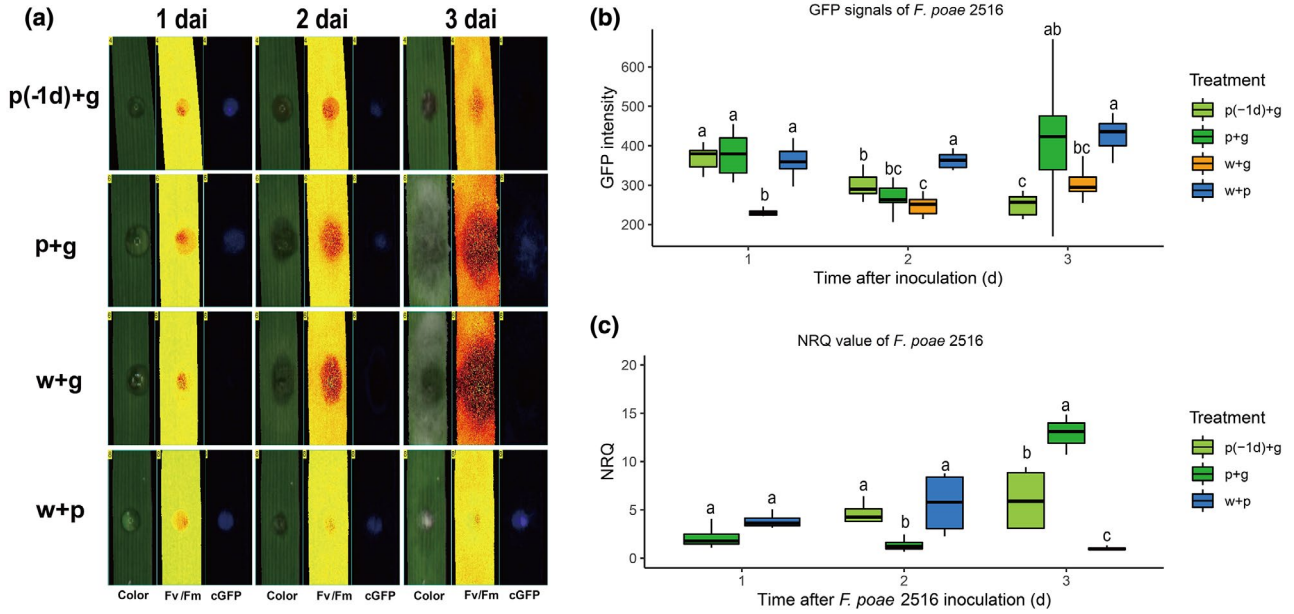

FIGURE 3 Impact of *Fusarium graminearum* PH-1 inoculation on *Fusarium poae* 2,516 infection in a detached leaf assay. (a) Green fluorescent protein-tagged *F. poae* 2,516 inoculation from 1 to 3 days after inoculation (dai). p(−1d) + g, preinoculation with *F. poae* 2,516 1 day before *F. graminearum* PH-1 inoculation; p + g, inoculation with *F. poae* 2,516 and *F. graminearum* PH-1 at the same time; w + g, inoculation of water and *F. graminearum* PH-1 at the same time; w + p, inoculation with water and *F. poae* 2,516 at the same time. (b) Corrected green fluorescent protein (GFP) value signal from 1 to 3 dai, $n = 8$. (c) Normalized quantitative relative values (NRQ) of *F. poae* 2,516 biomass on leaves, $n = 4$. Boxplots indicate the median (horizontal lines), 25th and 75th percentile range (boxes), and up to 1.5× interquartile range (whiskers). Different letters indicate significant differences between treatments ($p < .05$) for each time point

using liquid chromatography coupled to mass spectrometry (LC-MS/MS) (Figures 5 and S10). In detached leaves, the singular *F. graminearum* infection resulted in the highest DON level, with a mean concentration of 69 mg/kg, followed by the coinoculation treatment of *F. poae* and *F. graminearum* at 45 mg/kg. All these treatments resulted in median DON concentrations of more than 20 mg/kg of leaf material. Preinoculation of leaves with *F. poae* 1 day before *F. graminearum* resulted in a significantly lower concentration of DON (3.1 mg/kg) compared to singular *F. graminearum* inoculations (Student's *t* test, $p = .011$). Also, for the DON metabolite 15-ADON, lower concentrations were found if leaves were inoculated with *F. poae* 1 day before *F. graminearum* (1.2 mg/kg) compared to singular *F. graminearum* inoculations (2.4 mg/kg). For 3-ADON concentrations were relatively low 0.6 mg/kg compared to 1.0 mg/kg, and were similar in all treatments irrespective of the coinoculation with *F. poae*. As PH-1 is a 15-ADON chemotype (Alexander *et al*., 2011), thus not a 3-ADON producer, these trace levels may be attributed to spontaneous chemical conversion of 15-ADON to 3-ADON. DON-3G is generated by plants via a detoxifying mechanism, where a glucose moiety is added to DON. The highest DON-3G concentration was observed in interactions were *F. graminearum* was inoculated alone or in simultaneous coinoculations with *F. poae* (Figures 5b and S10).

A similar approach was pursued in wheat ears. All DON concentrations of wheat ears inoculated by *F. graminearum* or simultaneously inoculated with *F. poae* and *F. graminearum* resulted in similar DON levels of around 12 mg/kg. Preinoculation of ears with *F. poae* 1 day before *F. graminearum* resulted in significant reduction of the DON concentration (5.5 mg/kg) compared to singular *F. graminearum* inoculations (12.8 mg/kg, Student's *t* test, $p = .01$). Also, for the DON metabolite 15-ADON lower concentrations were found if ears were inoculated with *F. poae* 1 day before *F. graminearum* (0.4 mg/kg) compared to singular *F. graminearum* inoculations (0.6 mg/kg). For 3-ADON concentrations were relatively low, 0.07 mg/kg compared to 0.14 mg/kg, and similar in all treatments irrespective of the coinoculation with *F. poae*. The highest DON-3G concentration was observed in interactions where *F. graminearum* was inoculated alone or in simultaneous coinoculations with *F. poae* (Figures 5d and S10).

We quantified the presence of NIV, FUS-X, NEO, and DAS in both detached leaves and ears. Surprisingly, none of these trichothecenes were detected in any of the samples, indicating levels below the limit of detection (NIV 30 μg/kg, FUS-X 31 μg/kg, NEO 39 μg/kg, and DAS 41 μg/kg).

2.5 | Effect of *F. poae* and *F. graminearum* infection on SA and JA responses, and PR-gene expression in detached wheat leaves and ears

To study the impact of a singular *F. graminearum* or *F. poae* infection on the SA and JA responses in detached leaves and ears, we analysed the expression level of genes encoding hallmark enzymes phenylalanine ammonia-lyase (*PAL*) and isochorismate synthase (*ICS*) for the SA biosynthesis, and lipoxygenases *LOX1* and *LOX2* for the biosynthetic pathway leading to JA.

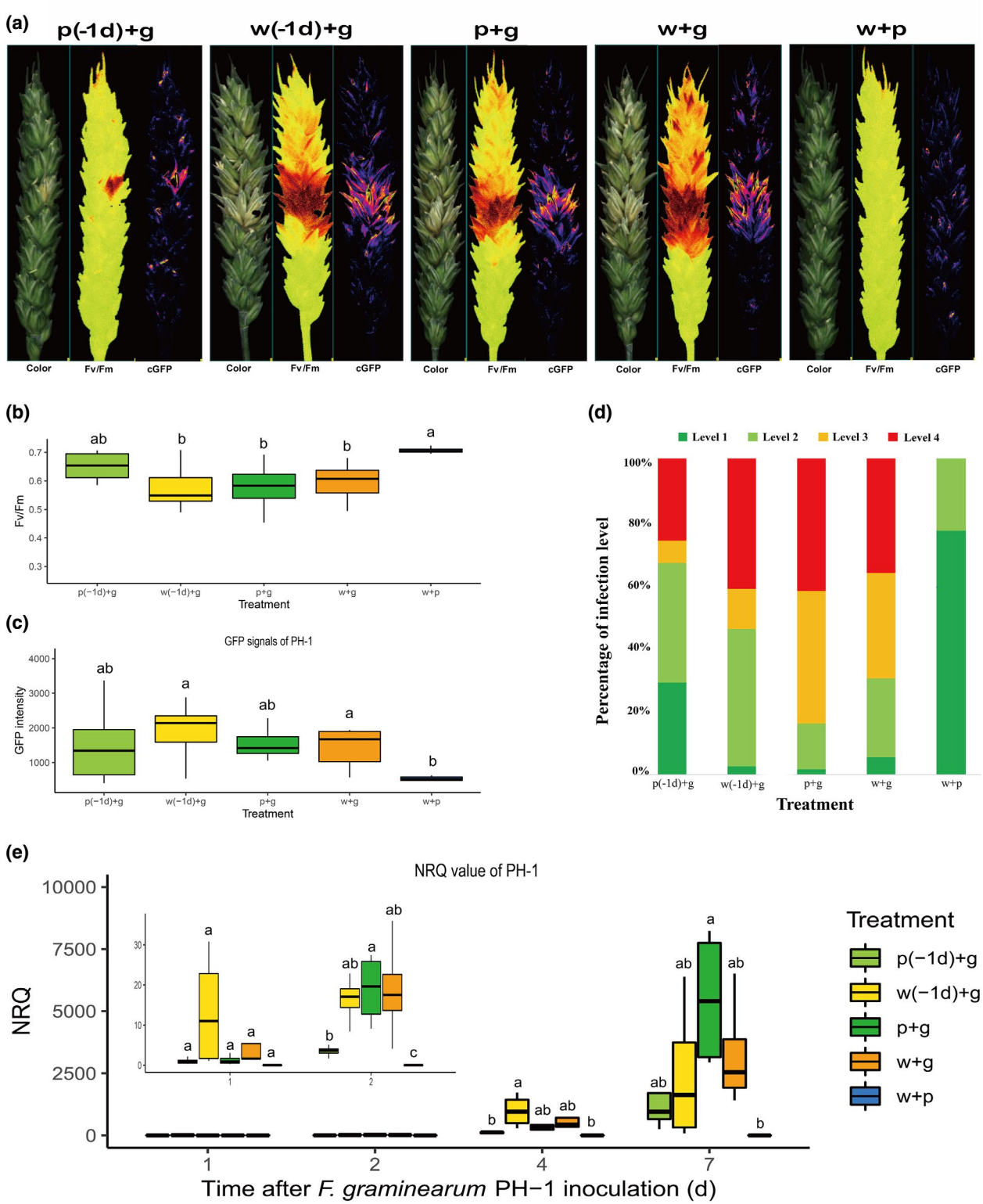

FIGURE 4 Impact of *Fusarium poae* 2,516 inoculation on *Fusarium graminearum* PH-1 infection on wheat ears. (a) Representative pictures taken at 7 days after inoculation (dai). p(−2d) + g, preinoculation with *F. poae* 2,516 2 days before *F. graminearum* PH-1 inoculation; w(−2d) + g, preinoculation with water 2 days before *F. graminearum* PH-1 inoculation; p(−1d) + g, preinoculation of *F. poae* 2,516 1 day before *F. graminearum* PH-1 inoculation; w(−1d) + g, preinoculation of water 1 day before *F. graminearum* PH-1 inoculation; p + g, inoculation with *F. poae* 2,516 and *F. graminearum* PH-1 at the same time; w + g, inoculation with water and *F. graminearum* PH-1 at the same time; w + p, inoculation with water and *F. poae* 2,516 at the same time. (b) F_V/F_M (efficiency of photosystem II) values at 7 dai, $n = 8$. (c) Corrected green fluorescent protein (GFP) value from the GFP expressing *F. poae* 2,516 mutant signal at 7 dai, $n = 8$. (d) Infection level after 7 dai. (e) Normalized quantitative relative values (NRQ) of *F. graminearum* PH-1 biomass at 1, 2, 4, and 7 dai, $n = 4$. Boxplots indicate the median (horizontal lines), 25th and 75th percentile range (boxes), and up to 1.5× interquartile range (whiskers). Different letters indicate significant differences between treatments ($p < .05$) for each time point

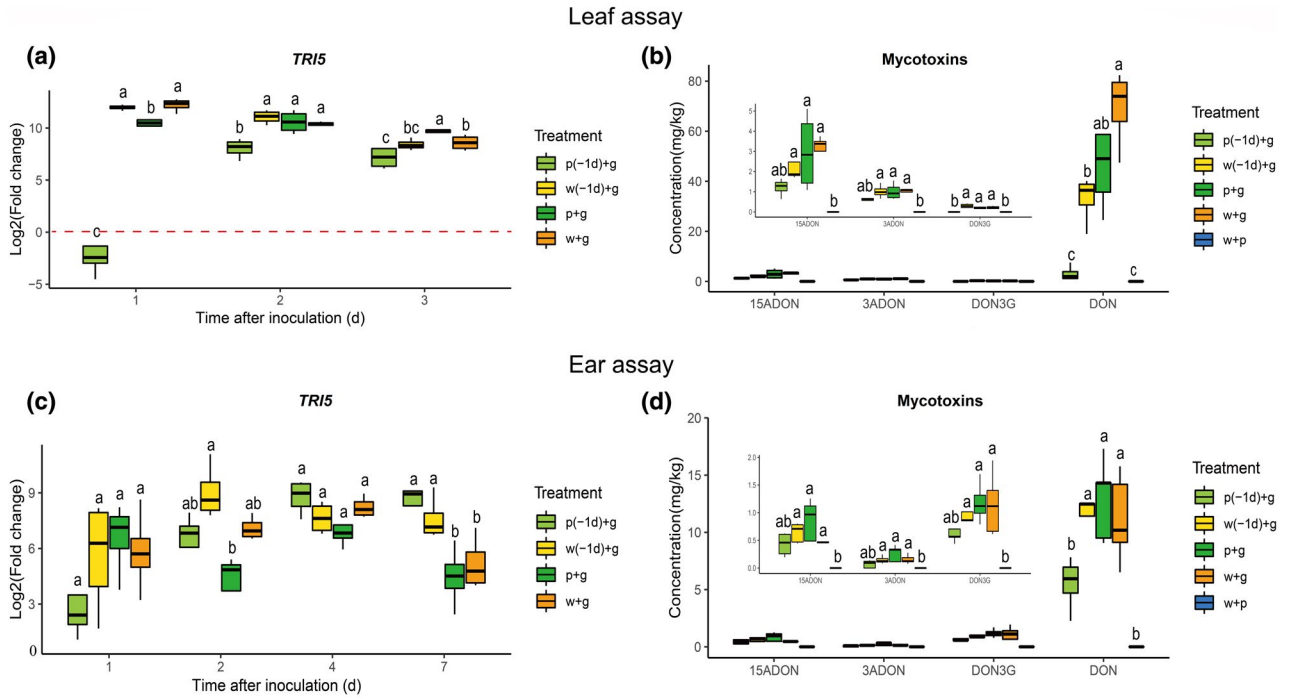

FIGURE 5 Impact of *Fusarium poae* 2,516 on mycotoxins produced by *Fusarium graminearum* PH-1. (a) Expression profile of the *TRI5* gene in *F. graminearum* PH-1 during a period of 3 days on wheat leaves. Data represent four biological replicates. The expression of the *TRI5* gene from *F. poae* is below detection level as the 2,516 biomass is very low. (b) Mycotoxin concentrations 4 days after inoculation of wheat leaves with *F. graminearum* PH-1. Data represent four biological replicates. (c) Expression profile of the *TRI5* gene in *F. graminearum* PH-1 during a period of 7 days on wheat ears. Data represent four biological replicates. The expression of *TRI5* gene in *F. poae* is below detection level as the biomass is very low. (d) Mycotoxin concentrations 7 days after inoculation on wheat ears with *F. graminearum* PH-1. Data represent five biological replicates. Boxplots indicate the median (horizontal lines), 25th and 75th percentile range (boxes), and up to 1.5× interquartile range (whiskers). Different letters indicate significant differences between treatments ($p < .05$) for each time point

In the detached leaf assay, *F. graminearum* infection (w[−2d] + g, w[−1d] + g, and w + g) resulted in a trend of *PAL* up-regulation (Figure S11a) and a down-regulation of *ICS* (Figure S11b) at all measured time points. For *LOX2*, a down-regulation was observed at days 2 and 3 in w + g, and at days 1 and 3 in w(−1d) + g (Figure S11d), while the expression of *LOX1* was up-regulated in w(−1d) + g and w + g at day 1, and w(−2d) + g and w(−1d) + g at day 3 compared to the control (w[−2d] + w, w[−1d] + w, and w + w; Figure S11c).

Infection with *F. poae* (w + p) resulted in a completely different profile of the SA and JA primary biosynthesis genes. An early induction of both *LOX1* and *LOX2* trends was observed at 1 day after inoculation (Figure S11c,d). In addition, a transient induction of *ICS* was observed at 2 days after inoculation (Figure S11b). These results show that although *F. poae* does not cause any symptoms, it does induce defence responses in detached leaves.

In addition, we also assessed the expression profiles of three important pathogenesis-related (PR) genes (*PR1*, *PR4*, and *PR5*) as well as peroxidase (*PEROX*). Despite the fact that *F. poae* did not cause symptoms in detached leaves, a clear and consistent induction of all three PR genes was observed at all time points (Figure S11f–h). *PEROX*, which constitutes an early response to pathogens, showed a transient induction in response to *F. poae* alone (Figure S11e). These genes were also induced by *F. graminearum*, although the expression levels were higher in the latter interaction.

In wheat ears, the infection of *F. graminearum* (w[−2d] + g, w[−1d] + g, and w + g) resulted in a trend of consistently higher induction of *PAL* in the first 7 days (Figure 12a) while *ICS* was suppressed at all time points (Figure S12b). For *LOX1* and *LOX2*, no clear effects were observed at days 1 and 2 but a suppression of *LOX2* was observed at days 4 and 7 (Figure S12c,d). This response was highly similar to the *F. graminearum* response in the detached leaf assay, which shows that the detached leaf assay is an adequate high-throughput alternative for wheat ear infections (Figure S11c,d). The infection with *F. poae* (w + p) resulted in an up-regulation of *PAL* from day 1 onwards except for day 2 (Figure S12a). In addition, *LOX1* (Figure S12c) and *ICS* (Figure S12b) were induced at days 2 and 7, respectively. Similar to the response in the detached leaf assay, the expression profiles of three important PR genes (*PR1*, *PR4*, and *PR5*) and *PEROX* showed a clear and consistent induction at all time points in both *F. poae* and *F. graminearum* (Figure S12e–h).

2.6 | Defence response after dual infection of detached wheat leaves and wheat ears with *F. poae* and *F. graminearum*

When *F. poae* was inoculated on detached wheat leaves 1 or 2 days before the *F. graminearum* infection (p[−2d] + g and p[−1d] + g), no

suppression of *ICS* or *LOX2*, which was characteristic of an inoculation with *F. graminearum* alone (w[−2d] + g and w[−1d] + g), was observed. On the contrary, in the treatments in which *F. poae* was preinoculated 1 or 2 days before *F. graminearum* (p[−2d] + g and p[−1d] + g), a slight induction of *PAL* and *ICS* was observed 2 days after the *F. graminearum* infection (which was 3 days after the *F. poae* infection; Figure S11). Finally, when we preinoculated *F. graminearum* before *F. poae* (g[−1d] + p), expression of the defence genes *PAL*, *PR1*, *PR4*, *PR5*, and *PEROX* was higher than the singular *F. poae* infection, while *ICS* was relatively lower (Figure S13).

The kinetics of the gene expression were more complex in wheat ears compared to wheat leaves. First of all, the singular inoculation with *F. graminearum* or the simultaneous inoculation of *F. graminearum* at the same time as *F. poae* resulted in a reduction in the expression of *ICS* at days 4 and 7. This reduction was less pronounced when *F. poae* was preinoculated 1 day before *F. graminearum*. In regard to expression of *LOX1*, the induction that was observed in detached wheat leaves upon *F. poae* inoculation was confirmed in wheat ears: singular *F. poae* inoculation and *F. poae* inoculation 1 day before *F. graminearum* inoculation resulted in an up-regulation of *LOX1* while singular *F. graminearum* inoculation resulted in a down-regulation of *LOX1*. Similar to detached wheat leaves, all treatments except for the control treatments resulted in an induction of *PR1*, *PR4*, *PR5*, and *PEROX* (Figure S9e–h). The induction of these genes, especially of *PEROX*, was higher in interactions in which *F. graminearum* was inoculated alone compared to interactions in which *F. poae* was inoculated alone or in which *F. poae* was inoculated 1 day before *F. graminearum*.

2.7 | Principal component analysis of gene expression, fungal biomass cGFP and NRQ, and the health condition of the plant (F_V/F_M)

To study whether enhanced defence against *F. graminearum* might play a role after preinoculation with *F. poae*, we performed a principal component analysis (PCA) on defence gene expression data, combined with multispectral data accounting for the fungal biomass (cGFP and normalized quantitative relative values [NRQ]) and the health condition of the plant (F_V/F_M) in both the leaf and ear assays.

In detached leaves at day 1 the control treatments (w[−2d] + w, w[−1d] + w, or w + w) clustered, were clearly distinct from all other treatments, and were separated along the first principal component. Analysis of the factor loadings (component coefficients) showed that the singular *F. poae* infection positively associated with the expression of *LOX1* (lipoxygenase1) and *LOX2* (lipoxygenase2). As the disease progressed, at days 2 and 3, several patterns emerged. The singular *F. graminearum* inoculations or the treatments in which *F. graminearum* was simultaneously applied with *F. poae* could be differentiated along the first principal component from all other treatments. The singular *F. poae* inoculations and the inoculations in which *F. poae* was applied 1 or 2 days before *F. graminearum* were more closely related to the control treatment. Analysis of the loading factors shows that *ICS* and *LOX2* were positively correlated with F_V/F_M and contributed to the separation along the first principal component. Furthermore, the amount of fungal biomass as indicated by the cGFP signal and NRQ were negatively correlated with F_V/F_M, *ICS*, and *LOX2* (Figures 6 and S14, and Table S1).

In ears, similar to leaf assay, from day 1 the control treatments clustered and were clearly distinct from all other treatments, and were split along the first principal component axis. Analysis of the factor loadings showed that the infection positively correlated with the expression of *LOX1* and *ICS* and negatively correlated with the expression of *LOX2* and *PAL* at day 1. At days 2, 4, and 7 control treatments, singular *F. poae* inoculations and inoculations in which *F. poae* was applied 1 or 2 days before *F. graminearum* infections could be separated from the other treatments along the first principal component. Analogously as in the leaf assay, a positive correlation was observed in these treatments with *LOX1* or *LOX2* and *ICS* gene expression (Figures 7 and S15, and Table S1).

3 | DISCUSSION

In plant pathology, the interaction of a plant with an invading pathogen is often considered as a bidirectional interaction involving a single pathogenic strain and its host. The outcome of this interaction is then typically determined by the mutual interplay of plant- and pathogen-derived signals and pathways.

Yet, in some of the world's most important fungal plant diseases, several species or genera have been isolated from the tissue with symptoms, which suggests that multiple species and/or genera are involved in the cause and/or development of the disease (Lamichhane and Venturi, 2015). FHB in wheat can be caused by a complex of *Fusarium* species, black sigatoka disease in banana is caused by several *Mycosphaerella* species (Arzanlou *et al*., 2007), leaf spot on *Eucalyptus* is caused by several *Teratosphaeria* species (Crous *et al*., 2009), and potato leaf spot is caused by a complex of *Alternaria* species (Vandecasteele *et al*., 2018). Sometimes even different fungal genera are involved in one disease, for example grapevine decline caused by Botryosphaeriaceae spp. and Ilionectriaceae spp. (Whitelaw-Weckert *et al*., 2013) and rice sheath rot disease caused by *Fusarium* spp. and *Sarocladium oryzae* (Bigirimana *et al*., 2015). *Aphanomyces euteiches* is an important root rot pathogen in pea. Despite the fact that *Fusarium solani* does not cause symptoms in pea, coinoculation of plants with *A. euteiches* and *F. solani* resulted in significantly greater disease severity than *A. euteiches* alone, which points to a synergistic action of both fungi in the interaction with the plant (Peters and Grau, 2002).

Sometimes, even interkingdom associations are formed. As such, infection of maize by *F. verticillioides* is facilitated by the European corn borer (*Ostrinia nubilalis*; Blandino *et al*., 2015). The former synergistic action of an insect and a fungus causing a disease is not due to the insect vectoring the fungus. On the contrary, the European corn borer damages the maize plant and these wounds are used by *F. verticillioides* as entry points. Studies focused on these types of

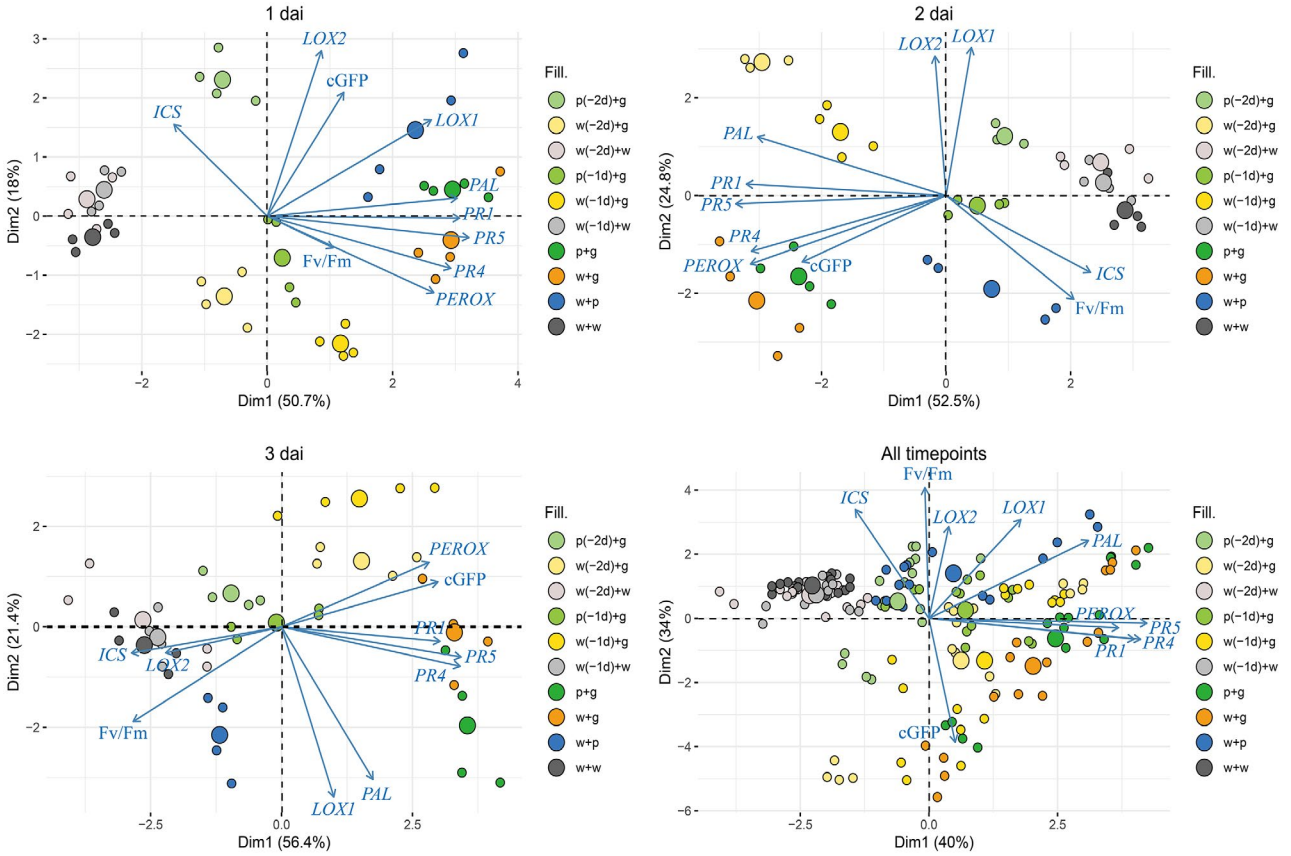

FIGURE 6 Principal component analysis of gene expression, fungal biomass corrected green fluorescent protein (GFP) value from the GFP-expressing PH-1 mutant, and normalized quantitative relative values, and the health condition of the plant (F_V/F_M [efficiency of photosystem II]) from 1 to 3 days after inoculation (dai) and all time points in leaf assay. Data show the control treatments cluster separately from the w + g, p + g, w(−1d) + g, and w(−2d) + g treatments along the first principal component. The w + p, p(−1d) + g, and p(−2d) + g treatments are more closely related to the control treatment. Analysis of the factor loadings shows that F_V/F_M, *ICS*, and *LOX2* are positively correlated and contribute to the separation along the first principal component. The size of the circles is proportional to their cos2 value

fungal diseases are still in their infancy and the available papers are often limited to the interaction of one member of the disease complex (often the most virulent one or the most frequently encountered one) with the host or focus on the identification of new species or genera in a disease complex (Lamichhane and Venturi, 2015, and the references therein).

Within the many different species involved in FHB, we aspired to unravel in detail the interaction between two predominant FHB species of wheat in Europe: the virulent pathogen *F. graminearum*, which often co-occurs with the weak pathogen *F. poae*. Their co-occurrence in several countries throughout Europe is counterintuitive as they behave quite differently on wheat ears. *F. graminearum* infects directly or infects through natural openings, after which it grows under the cuticle along stomatal rows (Pritsch *et al.*, 2000). Subsequently, it colonizes glumal parenchyma cells. When it finally migrates to the rachilla and rachis, it starts to produce the necrotizing molecule DON (Audenaert *et al.*, 2014). *F. poae*, on the other hand, is a weak pathogen that causes minor symptoms and infection is limited to the glumae (Siou *et al.*, 2015). Despite their different lifestyles, they share the same host and ecological niche at the onset of infection, which leads to the assumption that they may interact with each other.

Using two model infection systems on detached leaves as well as on ears of intact plants, we observed that coinoculation of *F. graminearum* with the weak pathogen *F. poae* did not differ significantly from a singular *F. graminearum* infection. However, when detached leaves or ears were preinoculated with *F. poae* 1 day before *F. graminearum* infection, a clear reduction in disease symptoms was observed. In addition, we looked at the active fungal biomass by performing RT-qPCR analyses and monitoring the cGFP signal. Both inoculation assays showed that *F. graminearum* abundance was reduced when preinoculated with *F. poae*, while *F. poae* benefitted from the presence of *F. graminearum*, resulting in a small but consistent increase in its biomass compared to a single *F. poae* inoculation. We assumed that *F. poae* benefits from the increased amount of damaged tissue caused by the aggressive pathogen *F. graminearum* to expand on wheat. To confirm our hypothesis, we inoculated the GFP-tagged *F. poae* on mechanically wounded leaves. *F. poae* showed more extensive growth in larger wounds, advocating a more saprophytic role for *F. poae* in the disease complex. It should be noted that in this study we used single isolates of *F. graminearum* and *F. poae*, which means that the obtained results may be isolate-specific.

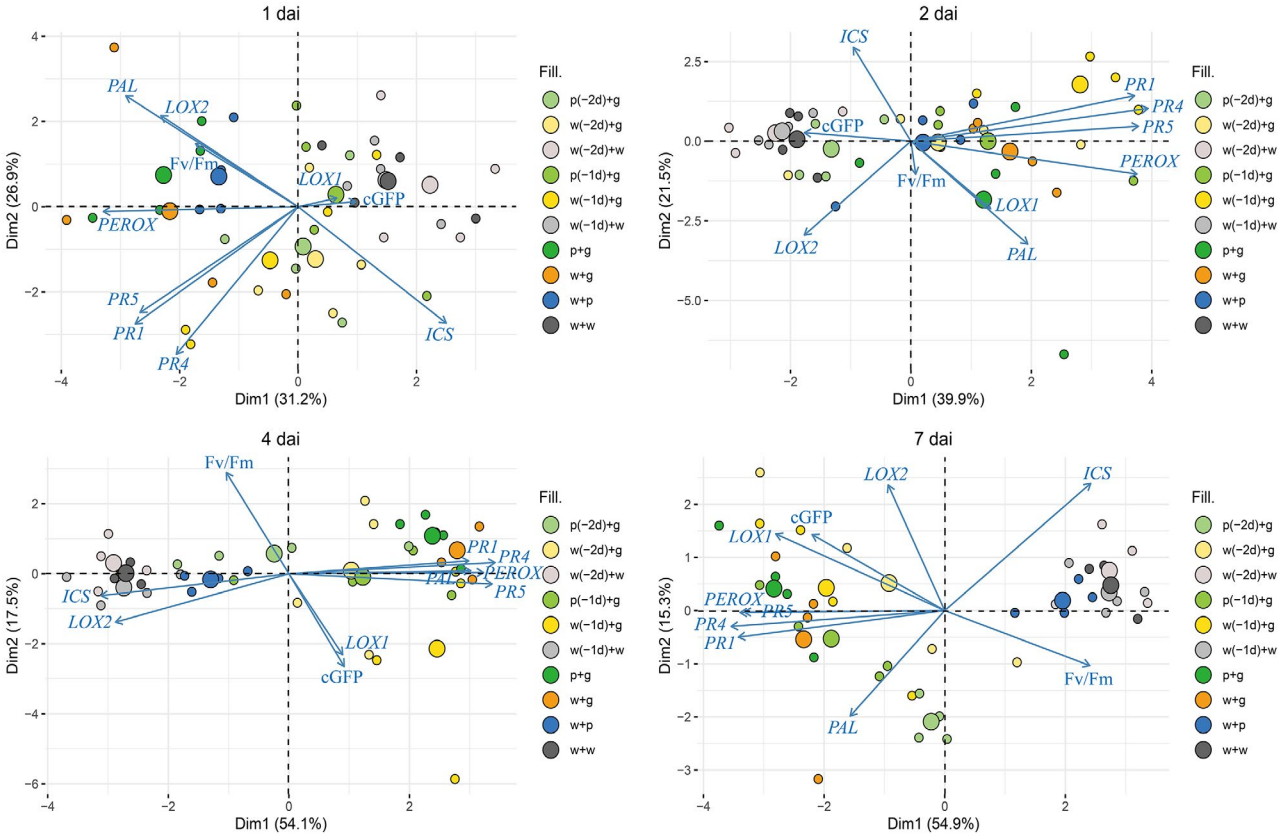

FIGURE 7 Principal component analysis of gene expression, fungal biomass corrected green fluorescent protein value, and normalized quantitative relative values, and the health condition of the plant (F_V/F_M [efficiency of photosystem II]) at 1, 2, 4, and 7 days after inoculation (dai) in ear assay. Data show the control treatments cluster separately from the w + g, p + g, w(−1d) + g, and w(−2d) + g treatments along the first principal component. The w + p and p(−1d) + g treatments are more closely related to the control treatment. A positive correlation was observed in these treatments with *LOX1* or *LOX2* and *ICS* gene expression. The size of the circles is proportional to their cos2 value

In a paper by Pirgozliev *et al.* (2012) the interaction between *Microdochium* spp. and *F. culmorum* was investigated, and they reported on increased FHB symptoms and DON accumulation when wheat heads were preinoculated by the more saprophytic *Microdochium* spp. followed by *F. culmorum*. Because DON is produced on stress, it was suggested that the competition for space and nutrients attributed to the increase in DON resulted in increased FHB. On the other hand, Xu *et al.* (2007) found no synergistic interactions for FHB pathogen coinoculations. However, competition between *Fusarium* isolates was reported in which *F. graminearum* was most competitive in dual inoculation with *F. poae*, *F. culmorum*, and *F. avenaceum*, where these latter pathogens had significantly less fungal biomass compared to single inoculations. More recently, Siou *et al.* (2015) highlighted a possible interaction between *F. poae* and *F. graminearum*, stating that the colonization of wheat by *F. poae* in the centre of the ear hampered the infection by *F. graminearum* inoculated three spikelets higher. This study highlighted the possible antagonistic effects of *F. poae* against *F. graminearum*, but did not further investigate the underlying mechanisms.

To explain the observations from this study, we first assessed the direct antagonism between *F. poae* and *F. graminearum* by coculturing them in vitro. However, coinoculation of both species on PDA plates did not uncover any mutual antagonism (Figure S5). Although different conditions were used, this observation was in slight contrast to previous reports showing that the weak pathogen *F. poae* did not influence the in vitro growth and germination of *F. graminearum* while the latter one outcompeted *F. poae* in a confrontation assay (Wagacha *et al.*, 2012).

We further explored the interaction between *F. poae* and *F. graminearum*, hypothesizing that *F. poae* and *F. graminearum* interact during the infection of wheat at the level of their trichothecenes. This hypothesis originates from the fact that DON is a crucial virulence factor during the spread of *F. graminearum* in the rachilla and the rachis (Audenaert *et al.*, 2014). In addition, it is known that *F. poae* produces a much more diverse blend of mycotoxins comprising both type A and type B trichothecenes (Vanheule *et al.*, 2017). Therefore, we wanted to investigate whether precolonization of wheat ears or detached leaves with the weak pathogen *F. poae* resulted in accumulation of *F. poae*-specific mycotoxins like NIV, DAS, and NEO, which in turn could affect the growth and colonization of *F. graminearum*. However, none of the *F. poae* trichothecenes could be detected during the colonization of detached leaves or wheat ears, despite the fact that in previous research we have already shown isolate 2,516 to be a DAS and NEO producer (Vanheule *et al.*, 2017), which suggests that these toxins serve other purposes and are not involved in the competition for niche in the FHB disease complex. The situation

was different for *F. graminearum*, as preinoculation of *F. poae* resulted in a reduced presence of 15-ADON and DON compared to single *F. graminearum* inoculations. This reduced amount of type B trichothecenes in mixed inoculations could be attributed to a lower amount of *F. graminearum* biomass but not to a reduced production per biomass.

As trichothecene production could not explain the antagonistic effect of *F. poae* preinoculation on colonization by *F. graminearum*, we hypothesized that a plant-mediated response induced by preinoculation of *F. poae* might hamper a later *F. graminearum* infection. The activation of plant defence in tomato by Fo47, a nonpathogenic strain of *F. oxysporum* against a pathogenic *F. oxysporum* strain, has already been demonstrated (Fuchs *et al*., 1997; Aimé *et al*., 2013). Moreover, this was not only limited to strains from the same species of a single genus as Fo47 could also protect against *Pythium ultimum* in cucumber by inducing host plant defence responses (Benhamou *et al*., 2002).

Pursuing a more holistic approach, we combined multispectral and gene expression data in a PCA. By monitoring crucial wheat defence genes, we showed that a single *F. graminearum* infection and coinoculation of *F. graminearum* and *F. poae* resulted in a consistent down-regulation of SA or JA defence pathways through down-regulation of *LOX* and *ICS* genes. In contrast, and although *F. poae* does not induce symptoms, a sequential up-regulation of *ICS* and *LOX* genes was observed at several time points after the inoculation. We hypothesize that the early induction of SA- and JA-related defences by *F. poae* hampers a subsequent *F. graminearum* infection. Previously, we have shown, using a priming approach with the green leaf volatile *Z*-3-hexenyl acetate, that a successful defence of wheat against *F. graminearum* is sequentially and meticulously regulated by SA and JA during the early stages of infection (Ameye *et al*., 2015). Similarly, preinoculation of detached leaves or wheat ears with a weak pathogen such as *F. poae* modifies this meticulously regulated system of the plant's innate defence. Similar results were obtained in a different study in which we investigated an interkingdom interaction between wheat, *F. graminearum*, and *Sitobion avenae* (English grain aphid; De Zutter *et al*., 2017). In that work, preinfestation of wheat ears with aphids resulted in down-regulation of *PAL* at early time points, which resulted in suppression of *PAL* during a subsequent *F. graminearum* infection compared to a single *F. graminearum* infection and a more proliferated outgrowth of the fungal pathogen (De Zutter *et al*., 2017).

Together our results highlight the importance of temporal dynamics between different members of the same disease complex in that the timing of infection shapes the outcome of symptom development and pathogen survival by extension.

4 | EXPERIMENTAL PROCEDURES

4.1 | *Fusarium* spp. survey

The FHB population on winter wheat was surveyed during all growing seasons between 2002 and 2018 in seven locations situated in the main wheat-growing regions of Flanders. In each growing season a total of 10 popular commercial varieties were included in the FHB survey, using a randomized block design with at least three replications providing a total of 210 fields per year, where plot size varied between 15 and 25 m^2. The locations of these fields are reported in Audenaert *et al*. (2009). Conventional crop management was practised, including three nitrogen fertilizations according to the N-index established by the soil service of Belgium (Geypens *et al*., 1994) and pre- and postemergence herbicide applications. One fungicide treatment was applied at growth stage (GS) 59. The fungicide treatment (epoxyconazole [75 g/ha] and kresoxim-methyl [125 g/ha]) was not targeted against *Fusarium* spp. but was included to control other leaf and ear diseases.

Two weeks after anthesis, two diseased ears were selected per field for assessing the presence of *Fusarium* spp., which resulted in 420 samples per year. Individual spikelets with symptoms were plated and outgrowing fungi and monospore isolates were prepared. The species used in present study were identified by PCR and/or *EF1* sequencing as previously described in Audenaert *et al*. (2009).

4.2 | *Fusarium* strains and transformation of *F. graminearum* and *F. poae*

F. graminearum PH-1 (Trail and Common, 2000) and *F. poae* 2,516 (Vanheule *et al*., 2016) were used throughout the study. The GFP-encoding gene together with promoter was amplified from plasmid pRFHUE-GFP (addgene: #89469). The amplified fragments were inserted after *hygromycin B* of the plasmid vector pII99 between the cut sites of restriction enzymes *Hin*dIII and *Sac*I (Thermo Scientific; Figure S16). Transformation of *F. graminearum* and *F. poae* was adjusted from Ammar *et al*. (2013) and performed as described in Methods S1. After transformation, the fitness of the transformant was assessed at the level of vegetative growth and sporulation, and additional virulence assessed for *F. graminearum*. No differences were observed when comparing with the wild type (Figure S17).

4.3 | Fungal growth, production, and isolation of conidia

The GFP transformants of *F. graminearum* PH-1 or *F. poae* 2,516 were grown on PDA for 7 days at 21°C under a regime of 12 hr of dark and 12 hr of combined UVA and UVC light (2 × TUV 8 W T5 and 1 × TL 8 W BLB; Philips). The transformants of *F. graminearum* PH-1 and *F. poae* 2,516 had no difference in fitness and/or virulence compared to the wild-type strains (Figure S17). Conidia were harvested by adding a solution of sterile 0.01% (vol/vol) Tween 80 to the PDA plates and rubbing the mycelium with a Drigalski spatula. Four layers of sterile Miracloth were used to filter the conidia and remove the mycelium. The suspension was diluted to a final concentration of 10^6 conidia/ml. This suspension was used for inoculations on both wheat leaves and ears.

4.4 | Plant materials

For the leaf bioassay, spring wheat cv. Tybalt was grown in pots (4.5 cm diameter × 6.5 cm height) in a growth chamber (21°C, 16 hr:8 hr, light:dark) for 10 days. For the wheat ear bioassay, six spring wheat cv. Tybalt were grown in each pot (15 cm diameter × 30 cm height) under glasshouse conditions until GS 65.

4.5 | Detached leaf and ear inoculation assays

Leaf segments of 4 cm were cut from the tip of the leaves of 10-day-old seedlings. These leaves were placed on their abaxial surface in Petri dishes containing 0.5% (wt/vol) bacteriological water agar amended with 40 mg/L benzimidazole. The conidial suspension (2.5 μl) was deposited in the centre of the leaf segment, which was wounded using a sterile inoculation needle as previously described (Ameye *et al*., 2015).

Two parallel experiments were performed (Figure S18). (a) To assess the impact of *F. poae* on the infection by *F. graminearum*, detached leaves were infected with wild-type *F. poae* 1 day before *F. graminearum* infection (p[−1d] + g) or simultaneously infected with *F. poae* and *F. graminearum* (g + p). In control treatments *F. poae* was replaced with water, w(−1d) + g and w + g. (b) To assess the impact of *F. graminearum* inoculation on the *F. poae* infection, detached leaves were infected with *F. graminearum* 1 day before *F. poae* infection (g[−1d] + p) or simultaneously infected with *F. poae* and *F. graminearum* (g + p). In the control treatments, instead of an inoculation with *F. graminearum*, water was used: w(−1d) + p and w + p, respectively. The disease progress in the detached leaves was assessed using a multispectral phenotyping platform including excitation LEDs to visualize and quantify GFP for 3 days. To assess the impact of *F. graminearum* on the growth of *F. poae*, detached leaves were inoculated with GFP-tagged *F. poae* and wild-type *F. graminearum*. GFP-tagged *F. poae* was also inoculated on leaves that were mechanically wounded by scratching the epidermal layer over a length of 0.1, 1, and 2 cm with a sterile scalpel.

The same approach was pursued in the wheat ear trials using the same nomenclature. At GS 65, ears were inoculated with *F. graminearum*, *F. poae*, or a combination of both at different time points. We used a point inoculation strategy in which one spikelet of each ear was infected with 10 μl of conidial suspension. The disease progress was monitored using a multispectral phenotyping platform for 7 days. Visual scoring assessment of ears inoculation was performed at 7 days after inoculation (dai) using a five-class disease index, where level 1 = no symptoms visible, level 2 = one ear caryopsis has symptoms, level 3 = two ear caryopses have symptoms, level 4 = all ear caryopses on the inoculation site have symptoms, and level 5 = all ear caryopses have symptoms (Figure S19).

4.6 | Disease progress: multispectral phenomics

To assess disease progression in detached leaves and in wheat ears, we employed a custom-build multispectral phenotyping and microdispenser platform called the PathoViewer. This platform allows the visualization of diverse physiological traits in real time, based on specific absorption, reflection, and emission patterns at a high temporal and spatial resolution at 6 μm. A monochrome camera system, including a filter wheel, allows pixel-to-pixel capturing of RGB values, chlorophyll fluorescence (Chl), and GFP fluorescence. (CropReporter; Phenovation). This camera system was mounted on a Cartesian coordinate robot that was housed in an acclimatized environment of temperature, light, and humidity. The chamber was equipped with sun LED modules (SLMs) (Phenovation).

Fungal progress was assessed based on symptom development using the RGB image. In addition, the effect of disease on the efficiency of photosystem II (F_V/F_M) was assessed (Baker, 2008). Finally, the GFP signal of *F. graminearum* or *F. poae* was used as a hallmark for fungal presence. GFP signals were corrected for autofluorescence of senescing leaves and ears resulting in the corrected GFP value (cGFP).

Using this approach, images were taken on 1, 2, and 3 dai in the detached leaf assay. As the disease progress and symptom development were slower in the ears, images were taken on 1, 2, 4, and 7 dai.

Secondary metabolite production was assessed based on the production of the red pigment rubrofusarin, which is typically synthesized by the gene cluster consisting of the gene coding for polyketide synthase PKS12, *aurJ*, *aurF*, *gip1*, and the hypothetical gene FG02329.1 (Frandsen *et al*., 2006).

4.7 | RNA extraction and RT-qPCR

Total RNA from both detached leaves and ears was extracted using TRIzol reagent (Sigma-Aldrich) according to the manufacturer's instructions and subsequently quantified with a Quantus fluorometer (Promega). First-strand cDNA was synthesized using the GoScript reverse transcription system (Promega). Using GoTaq qPCR Master Mix (Promega), RT-qPCR analysis was performed using a CFX96 system (Bio-Rad) with the following thermal settings: 95°C for 2 min, 40 cycles of 95°C for 15 s, and 60°C for 1 min. Melting curve analysis was performed using a temperature profile of heating to 95°C at the rate of 0.5°C/s. The primers used for all genes are listed in Table S2. Normalization of defence genes was performed using the cell division control protein gene (Ta54227) in wheat as reference. Fungal biomass was quantified using a pre-mRNA slicing factor of *F. graminearum* (FGSG_01244) and *F. poae* (FPOA_01282) as described before (Ameye *et al*., 2015). *TRI5* gene detection primers designed specifically for *F. graminearum* (*FGSG_TRI5*) and *F. poae* (*FPOA_TRI5*) confirmed no cross-reactivity in the PCR. Gene expression analysis was performed using qBase + software (Biogazelle).

4.8 | Quantification of type A and type B trichothecenes in detached leaves and wheat ears

To investigate whether coinoculation of *F. poae* and *F. graminearum* on wheat seedlings and ears impact the mycotoxin production, 10

different mycotoxins produced by both *F. poae* and *F. graminearum* were screened using LC-MS/MS based on De Boevre *et al.* (2012) and the methods described in Methods S2.

4.9 | Statistical analysis

For statistical evaluation, PCA and plots generation, the R software v. 3.6.0 (R Core Team, 2019) and the packages ggplot2 (Wickham, 2016), factoextra (http://www.sthda.com/english/rpkgs/ factoextra), agricolae (de Mendiburu, 2014), carData, car (Fox and Weisberg, 2018), FSA (Ogle, 2017), and cooccur (Griffith *et al.*, 2016) were used. For multiple comparisons, the normality and homogeneity of variances was assessed by the Shapiro–Wilk and Levene tests, respectively. When conditions were met, an analysis of variance (ANOVA) was performed followed by a post hoc Tukey test. When the conditions for parametric analyses were not met, a nonparametric Kruskal–Wallis test was used followed by a pairwise comparison using a corrected Dunn's test. All analyses were run at a significance level of $\alpha = 0.05$. Two-way interactions and higher order interactions between *Fusarium* species were analysed using a simple straightforward log-linear model as described by Xu *et al.* (2005) assuming a Poisson sampling in each location. K-way and higher-order effects were determined to significance levels of $\alpha = 0.05$.

ACKNOWLEDGMENTS

This work was supported by a BOF doctoral fellowship of Ghent University.

DATA AVAILABILITY STATEMENT

The data that support the findings of this study are available from the corresponding author upon reasonable request.

ORCID

Maarten Ameye https://orcid.org/0000-0002-1861-2959
Mohamed F. Abdallah https://orcid.org/0000-0002-3903-6452
Kris Audenaert https://orcid.org/0000-0002-8791-1282

REFERENCES

Aimé, S., Alabouvette, C., Steinberg, C. and Olivain, C. (2013) The endophytic strain *Fusarium oxysporum* Fo47: a good candidate for priming the defense responses in tomato roots. *Molecular Plant-Microbe Interactions*, 26, 918–926.

Alexander, N.J., McCormick, S.P., Waalwijk, C., van der Lee, T. and Proctor, R.H. (2011) The genetic basis for 3-ADON and 15-ADON trichothecene chemotypes in *Fusarium*. *Fungal Genetics and Biology*, 48, 485–495.

Ameye, M., Audenaert, K., De Zutter, N., Steppe, K., Van Meulebroek, L., Vanhaecke, L. *et al.* (2015) Priming of wheat with the green leaf volatile Z-3-hexenyl acetate enhances defense against *Fusarium graminearum* but boosts deoxynivalenol production. *Plant Physiology*, 167, 1671–1684.

Ammar, G.A., Tryono, R., Döll, K., Karlovsky, P., Deising, H.B. and Wirsel, S.G. (2013) Identification of ABC transporter genes of *Fusarium graminearum* with roles in azole tolerance and/or virulence. *PLoS One*, 8, e79042.

Arzanlou, M., Abeln, E.C., Kema, G.H., Waalwijk, C., Carlier, J., Vries, I. *et al.* (2007) Molecular diagnostics for the Sigatoka disease complex of banana. *Phytopathology*, 97, 1112–1118.

Audenaert, K., Landschoot, S., Vanheule, A., Waegeman, W., De Baets, B. and Haesaert, G. (2011) Impact of fungicide timing on the composition of the Fusarium head blight disease complex and the presence of deoxynivalenol (DON) in wheat. In: Thajuddin, N. (Ed.) *Fungicides-Beneficial and Harmful Aspects*; London, UK: InTech, pp. 79–98.

Audenaert, K., Van Broeck, R., Bekaert, B., De Witte, F., Heremans, B., Messens, K. *et al.* (2009) Fusarium head blight (FHB) in Flanders: population diversity, inter-species associations and DON contamination in commercial winter wheat varieties. *European Journal of Plant Pathology*, 125, 445–458.

Audenaert, K., Vanheule, A., Höfte, M. and Haesaert, G. (2014) Deoxynivalenol: a major player in the multifaceted response of Fusarium to its environment. *Toxins*, 6, 1–19.

Backhouse, D. (2014) Global distribution of *Fusarium graminearum*, *F. asiaticum* and *F. boothii* from wheat in relation to climate. *European Journal of Plant Pathology*, 139, 161–173.

Baker, N.R. (2008) Chlorophyll fluorescence: A probe of photosynthesis in vivo. *Annual Review of Plant Biology*, 59, 89–113.

Benhamou, N., Garand, C. and Goulet, A. (2002) Ability of nonpathogenic *Fusarium oxysporum* strain Fo47 to induce resistance against *Pythium ultimum* infection in cucumber. *Applied and Environmental Microbiology*, 68, 4044–4060.

Bigirimana, V.de P., Hua, G.K.H., Nyamangyoku, O.I. and Höfte, M. (2015) Rice sheath rot: an emerging ubiquitous destructive disease complex. *Frontiers in Plant Science*, 6, 1066.

Blandino, M., Scarpino, V., Vanara, F., Sulyok, M., Krska, R. and Reyneri, A. (2015) Role of the European corn borer (*Ostrinia nubilalis*) on contamination of maize with 13 *Fusarium* mycotoxins. *Food Additives & Contaminants: Part A*, 32, 533–543.

Brennan, J., Fagan, B., Van Maanen, A., Cooke, B. and Doohan, F. (2003) Studies on in vitro growth and pathogenicity of European *Fusarium* fungi. *European Journal of Plant Pathology*, 109, 577–587.

Browne, R. and Cooke, B. (2005) Resistance of wheat to *Fusarium* spp. in an in vitro seed germination assay and preliminary investigations into the relationship with fusarium head blight resistance. *Euphytica*, 141, 23–32.

Brown, N.A., Urban, M., Van De Meene, A.M. and Hammond-Kosack, K.E. (2010) The infection biology of *Fusarium graminearum*: defining the pathways of spikelet to spikelet colonisation in wheat ears. *Fungal Biology*, 114, 555–571.

Bushnell, W., Hazen, B., Pritsch, C. and Leonard, K. (2003) Histology and physiology of Fusarium head blight. In: Kurt, J.L. & William, R.B. (Eds.), *Fusarium head blight of wheat and barley*. St Paul, MN: APS Press, pp. 44–83.

Crous, P.W., Groenewald, J.Z., Summerell, B.A., Wingfield, B.D. and Wingfield, M.J. (2009) Co-occurring species of *Teratosphaeria* on *Eucalyptus*. *Persoonia*, 22, 38–48.

De Boevre, M., Di Mavungu, J.D., Maene, P., Audenaert, K., Deforce, D., Haesaert, G. *et al.* (2012) Development and validation of an LC-MS/MS method for the simultaneous determination of deoxynivalenol, zearalenone, T-2-toxin and some masked metabolites in different cereals and cereal-derived food. *Food Additives & Contaminants: Part A*, 29, 819–835.

De Zutter, N., Audenaert, K., Ameye, M., De Boevre, M., De Saeger, S., Haesaert, G. *et al.* (2017) The plant response induced in wheat ears by a combined attack of *Sitobion avenae* aphids and *Fusarium graminearum* boosts fungal infection and deoxynivalenol production. *Molecular Plant Pathology*, 18, 98–109.

Desmond, O.J., Manners, J.M., Stephens, A.E., Maclean, D.J., Schenk, P.M., Gardiner, D.M. *et al.* (2008) The *Fusarium* mycotoxin deoxynivalenol elicits hydrogen peroxide production, programmed cell death and defence responses in wheat. *Molecular Plant Pathology*, 9, 435–445.

Fox, J. and Weisberg, S. (2018) *An R companion to applied regression*. Thousand Oaks: Sage Publications.

Frandsen, R.J., Nielsen, N.J., Maolanon, N., Sørensen, J.C., Olsson, S., Nielsen, J. *et al.* (2006) The biosynthetic pathway for aurofusarin in *Fusarium graminearum* reveals a close link between the naphthoquinones and naphthopyrones. *Molecular Microbiology*, 61, 1069–1080.

Fuchs, J.-G., Moënne-Loccoz, Y. and Défago, G. (1997) Nonpathogenic *Fusarium oxysporum* strain Fo47 induces resistance to fusarium wilt in tomato. *Plant Disease*, 81, 492–496.

Geypens, M., Vandendriessche, H., Bries, J. and Hendrickx, G. (1994) Experience with a nitrogen-index expert system: A powerful tool in nitrogen recommendation. *Communications in Soil Science and Plant Analysis*, 25, 1223–1238.

Griffith, D.M., Veech, J.A. and Marsh, C.J. (2016) cooccur: probabilistic species co-occurrence analysis in R. *Journal of Statistical Software*, *69*, 1–17.

Ioos, R., Belhadj, A., Menez, M. and Faure, A. (2005) The effects of fungicides on *Fusarium* spp. and *Microdochium nivale* and their associated trichothecene mycotoxins in French naturally infected cereal grains. *Crop Protection*, 24, 894–902.

Lamichhane, J.R. and Venturi, V. (2015) Synergisms between microbial pathogens in plant disease complexes: a growing trend. *Frontiers in Plant Science*, 6, 385.

Leplat, J., Friberg, H., Abid, M. and Steinberg, C. (2013) Survival of *Fusarium graminearum*, the causal agent of Fusarium head blight. A review. *Agronomy for Sustainable Development*, 33, 97–111.

de Mendiburu, F. (2014) *Agricolae: statistical procedures for agricultural research*. R package version 1. http://CRAN.R-project.org/package=agricolae

O'Donnell, K., Ward, T.J., Geiser, D.M., Kistler, H.C. and Aoki, T. (2004) Genealogical concordance between the mating type locus and seven other nuclear genes supports formal recognition of nine phylogenetically distinct species within the *Fusarium graminearum* clade. *Fungal Genetics and Biology*, 41, 600–623.

Ogle, D.H. (2017) *FSA: fisheries stock analysis*. R package version 0.8, 17, 636. https://github.com/droglenc/FSA

Parry, D., Jenkinson, P. and McLeod, L. (1995) Fusarium ear blight (scab) in small grain cereals—a review. *Plant Pathology*, 44, 207–238.

Peters, R. and Grau, C. (2002) Inoculation with nonpathogenic *Fusarium solani* increases severity of pea root rot caused by *Aphanomyces euteiches*. *Plant Disease*, 86, 411–414.

Pirgozliev, S., Ray, R., Edwards, S., Hare, M. and Jenkinson, P. (2012) Studies on the interactions between fungicides, *Alternaria tenuissima*, *Cladosporium herbarum* and *Microdochium spp.*, on fusarium head blight (FHB) development and deoxynivalenol (DON) concentration in grain caused by *Fusarium culmorum*. *Cereal Research Communications*, 40, 509–517.

Pritsch, C., Muehlbauer, G.J., Bushnell, W.R., Somers, D.A. and Vance, C.P. (2000) Fungal development and induction of defense response genes during early infection of wheat spikes by *Fusarium graminearum*. *Molecular Plant-Microbe Interactions*, 13, 159–169.

R Core Team. (2019) *R: A language and environment for statistical computing*. Vienna, Austria: R Foundation for Statistical Computing. http://www.R-project.org/

Siou, D., Gélisse, S., Laval, V., Suffert, F. and Lannou, C. (2015) Mutual exclusion between fungal species of the fusarium head blight complex in a wheat spike. *Applied and Environmental Microbiology*, 81, 4682–4689.

Stack, R.W. and McMullen, M.P. (1985) Head blighting potential of *Fusarium* species associated with spring wheat heads. *Canadian Journal of Plant Pathology*, 7, 79–82.

Sugiura, Y., Fukasaku, K., Tanaka, T., Matsui, Y. and Ueno, Y. (1993) *Fusarium poae* and *Fusarium crookwellense*, fungi responsible for the natural occurrence of nivalenol in Hokkaido. *Applied and Environmental Microbiology*, 59, 3334–3338.

Thrane, U., Adler, A., Clasen, P.-E., Galvano, F., Langseth, W., Lew, H. *et al.* (2004) Diversity in metabolite production by *Fusarium langsethiae*, *Fusarium poae*, and *Fusarium sporotrichioides*. *International Journal of Food Microbiology*, 95, 257–266.

Trail, F. and Common, R. (2000) Perithecial development by *Gibberella zeae*: a light microscopy study. *Mycologia*, 92, 130–138.

Vandecasteele, M., Landschoot, S., Carrette, J., Verwaeren, J., Höfte, M., Audenaert, K. *et al.* (2018) Species prevalence and disease progression studies demonstrate a seasonal shift in the *Alternaria* population composition on potato. *Plant Pathology*, 67, 327–336.

Vanheule, A., Audenaert, K., Warris, S., van de Geest, H., Schijlen, E., Höfte, M. *et al.* (2016) Living apart together: crosstalk between the core and supernumerary genomes in a fungal plant pathogen. *BMC Genomics*, 17, 670.

Vanheule, A., De Boevre, M., Moretti, A., Scauflaire, J., Munaut, F., De Saeger, S. *et al.* (2017) Genetic divergence and chemotype diversity in the fusarium head blight pathogen *Fusarium poae*. *Toxins*, 9, 255.

Vogelgsang, S., Beyer, M., Pasquali, M., Jenny, E., Musa, T., Bucheli, T.D. *et al.* (2019) An eight-year survey of wheat shows distinctive effects of cropping factors on different *Fusarium* species and associated mycotoxins. *European Journal of Agronomy*, 105, 62–77.

Vogelgsang, S., Sulyok, M., Bänziger, I., Krska, R., Schuhmacher, R. and Forrer, H.-R. (2008) Effect of fungal strain and cereal substrate on in vitro mycotoxin production by *Fusarium poae* and *Fusarium avenaceum*. *Food Additives and Contaminants*, 25, 745–757.

Wagacha, J.M., Oerke, E.-C., Dehne, H.-W. and Steiner, U. (2012) Interactions of *Fusarium* species during prepenetration development. *Fungal Biology*, 116, 836–847.

Whitelaw-Weckert, M., Rahman, L., Appleby, L., Hall, A., Clark, A., Waite, H. *et al.* (2013) Co-infection by Botryosphaeriaceae and *Ilyonectria* spp. fungi during propagation causes decline of young grafted grapevines. *Plant Pathology*, 62, 1226–1237.

Wickham, H. (2016) *ggplot2: elegant graphics for data analysis*. New York: Springer. https://ggplot2.tidyverse.org

Xu, X.-M., Parry, D., Nicholson, P., Thomsett, M., Simpson, D., Edwards, S. *et al.* (2005) Predominance and association of pathogenic fungi causing fusarium ear blight in wheat in four European countries. *European Journal of Plant Pathology*, 112, 143–154.

Xu, X.M., Monger, W., Ritieni, A. and Nicholson, P. (2007) Effect of temperature and duration of wetness during initial infection periods on disease development, fungal biomass and mycotoxin concentrations on wheat inoculated with single, or combinations of, *Fusarium* species. *Plant Pathology*, 56, 943–956.

SUPPORTING INFORMATION

Additional supporting information may be found online in the Supporting Information section.

How to cite this article: Tan J, Ameye M, Landschoot S, et al. At the scene of the crime: New insights into the role of weakly pathogenic members of the fusarium head blight disease complex. *Molecular Plant Pathology*. 2020;21:1559–1572. https://doi.org/10.1111/mpp.12996